Petroleum Science 23 (2026) 2017–2029

Contents lists available at ScienceDirect

Petroleum Science

journal homepage: www.keaipublishing.com/en/journals/petroleum-science

Original Paper

Preparation and performance evaluation of self-degrading core–shell structure temporary plugging agent

Jia-Rui Li [a], Ling Lin [a,*], Lei Li [a], Hao Lu [a], Cheng-Yuan Xu [b], Xin-Min Zhang [c], Wen Ren [d]

[a] College of Chemistry and Chemical Engineering, Southwest Petroleum University, Chengdu, 610500, Sichuan, China
[b] College of Petroleum and Natural Gas Engineering, Southwest Petroleum University, Chengdu, 610500, Sichuan, China
[c] Sichuan Guangya Polymer Chemical Co., Ltd., Chengdu, 610500, Sichuan, China
[d] CNPC Research Institute of Safety and Environment Technology, State Key Laboratory of Petroleum Pollution Control, Beijing, 102206, China

ARTICLE INFO

Article history:
Received 27 September 2025
Received in revised form
10 March 2026
Accepted 12 March 2026
Available online 14 March 2026

Edited by Yan-Hua Sun

Keywords:
Shielding temporary plugging
Self-degradation
Core–shell structure
Polylactic acid

ABSTRACT

Temporary plugging agents (TPAs) are widely used in oilfield development due to their self-removal after operations and their minimal effect on reservoirs. However, the current methods used to remove TPAs may damage the reservoir. To address this, a self-degradable TPA for 120 °C conditions was prepared and tested in this study. Using acrylamide (AM) as the base monomer, along with polyethylene glycol diacrylate (PEGDA) and *N*,*N*′-methylenebisacrylamide (MBA) as crosslinkers, a crosslinked shell was synthesized. The degradation time of this shell can be adjusted by changing the ratio of two crosslinking agents. The shell served as a shielding layer to encapsulate polylactic acid (PLA), thereby delaying the latter's degradation. Experimental results confirmed that the TPA had a core–shell structure and exhibited good compatibility with base slurry. At a concentration of 0.5%, it effectively reduced filtration volume of base slurry. Furthermore, the TPA showed favorable plugging performance and pressure-bearing capacity. As the ratio of the two crosslinking agents varied, the water absorption capacity of the TPA exhibited an increasing trend, and its degradation duration at 120 °C ranged from 60 to 72 h. FT-IR and SEM analyses revealed structural changes of the TPA in the degradation process. All test results demonstrated that degradation primarily occured through the cleavage of amide and ester bonds, leading to the rupture of crosslinking points.

1. Introduction

Well leakage is a common challenge in drilling operations, which seriously inhibits the drilling cycle and increases drilling costs. If handled improperly, it will not only increase drilling equipment wear, but also may trigger a series of complex downhole incidents such as wellbore collapse, blowouts, and stuck pipes (Sun et al., 2021; Bai et al., 2022a, 2022b; Liu et al., 2025). When drilling fluid invades the reservoir through leakage channels such as reservoir pores, it not only causes reservoir contamination and permeability damage but also affects productivity (Li et al., 2023). One of the effective methods to deal with well leakage is the use of plugging agents. Temporary plugging agents (TPAs) can bridge and accumulate in formation pores to form a plugging zone that effectively retards the invasion of drilling fluid. They can be removed under specific conditions to restore the reservoir seepage channel and do not cause long-term plugging and damage, which may be introduced by using traditional plugging agents.

The primary principle of the shielding temporary plugging technology is to artificially add solid particles to the drilling fluids (Guo et al., 2022; Chen et al., 2024). Driven by a positive pressure difference during drilling, various-sized solid particles in the drilling fluid are forced to enter the reservoir pore throats or narrow fractures in an instant. This forms a dense shielding plugging layer on the wellbore wall, preventing drilling fluid from invading farther into the zone and thereby avoiding further damage to oil and gas reservoirs (Chen et al., 2023; Dindoruk and Zhang, 2024). The key lies in the selection of temporary plugging materials, which should exhibit excellent plugging ability and also self-removal performance when exposed to the reservoir after a certain time (Zhao et al., 2020; Zhu et al., 2021a; Zhou et al., 2025).

* Corresponding author.
E-mail address: cowbolinling@aliyun.com (L. Lin).
Peer review under the responsibility of China University of Petroleum (Beijing).

https://doi.org/10.1016/j.petsci.2026.03.028

TPAs commonly used in oil and gas field development can be mainly classified into water-soluble TPAs, oil-soluble TPAs, acid-soluble TPAs, and degradable TPAs (Zhu et al., 2021b; Liu et al., 2023). Among them, water-soluble TPAs feature low solution viscosity and good fluidity after degradation, but are subject to shortcomings such as a slow plugging removal rate (Liu et al., 2020; Wu et al., 2023); oil-soluble TPAs have a narrow application range, making them unsuitable for high water-cut wells, and they also entail high production costs (Kang et al., 2023; Zhao et al., 2023); acid-soluble TPAs are widely used in the field, but the acid treatment method used in the process of plugging removal will cause a certain degree of damage to the reservoir (Cui et al., 2021; Tang et al., 2023). In recent years, with increasing attention to reservoir protection, degradable TPAs have become a research hotspot because of their minimal reservoir damage during the plugging removal process. The common types of degradable TPAs include solid particles, gels, fibers, and others. Among them, gel-based TPAs possess a three-dimensional network structure, which can be flexibly deformed under pressure after water absorption and swelling, filling leakage channels of different sizes and exhibiting superior adaptability to reservoir pore throats. In addition, the gel demonstrates excellent compatibility with drilling fluid and can be easily injected into the formation, effectively addressing the drawbacks of solid particles, which show poor sealing tightness due to their rigidity, low fiber dispersibility, and low strength (Zhai et al., 2020; Yu et al., 2022; Wang et al., 2024).

Polylactic acid (PLA), poly (lactic-co-glycolic acid) (PLGA), and starch are commonly used as self-degradable TPAs due to their favorable biodegradability and environmental friendliness. However, PLA exhibits high brittleness and poor stability under high temperatures (Elsawy et al., 2017; Zaaba and Jaafar, 2020; Tang et al., 2023; Zhao et al., 2024). PLGA entails high production costs (Xu et al., 2023), while starch demonstrates poor temperature resistance, necessitating composite modification (Gong et al., 2021). Moreover, all of the above self-degradable TPAs are in particulate forms with poor adaptability to pore throats, unable to conform to changes in pore throats through deformation as gels can. Zou et al. (2023) synthesized a liquid TPA, SDG, using acrylamide, acrylic acid, and *N*,*N*′-methylenebisacrylamide as raw materials, and its degradation time could be adjusted by changing the concentration of acrylic acid and degradation temperature. When the acrylic acid concentration exceeded 37.5%, the degradation time of SDG at 90–130 °C ranged from 10 to 105 h. In addition to the introduction of unstable monomers, many scholars have introduced unstable crosslinking agents to promote the degradation of TPA. Wang et al. (2022) synthesized a high-adhesion self-degradable gel using neopentyl glycol diacrylate (SEG) as a crosslinking agent. The gel was obtained by changing the monomer ratio, and its self-degradation, driven by the hydrolysis of ester groups, exhibited varying degradation times at 60–100 °C. Yang et al. (2023) used polyethylene glycol diacrylate as a crosslinking agent and introduced hydrophobic monomers and nanoparticles to adjust water swelling and degradation time. The plugging agent prepared exhibited a degradation time of 20 d at 80 °C, while the unmodified one had a degradation time of 5 d. Yang et al. (2024) availed of amides with lower hydrolysis reactivity than ester groups to prepare a crosslinking agent with resistance to heat and hydrolysis. By changing the concentration of the crosslinking agent, the degradation time of the gel at 90–130 °C was controlled within the range of 5–25 d. Driven by the hydrolysis of the amide structure at high temperature, the TPA was transformed from a viscoelastic solid to a low-viscosity liquid. Zhang et al. (2022) prepared a degradable preformed particle gel (DPPG) synthesized from polyethylene glycol diacrylate (PEGDA)with different molecular weights. The results indicated that at 34 °C, as the molecular weight of PEGDA from 1000 to 200 Da, the degradation time of DPPG increased from 40 to 210 min. Zhu et al. (2023) adopted alkenoic ester-type and alcohol ester-type crosslinking agents to prepare TPAs. The results showed that TPAs prepared by alcohol ester had superior swelling performance and longer degradation times. At 34 °C, the corresponding degradation times for different swelling ratios ranged from 80 to 360 min. In summary, gel-based degradable TPAs prepared with different crosslinking agents exhibit different properties. However, most studies have focused on the effect of a single crosslinker on degradation time, with limited investigation into the relationship between the ratio of crosslinkers and degradation time. By changing the ratio of crosslinkers, the degradation time can be adjusted while ensuring the stability of the gel.

Acrylamide (AM) acts as a polymerizable monomer with mild reaction conditions and excellent crosslinking reactivity. *N*,*N*′-methylenebisacrylamide (MBA) forms a stable three-dimensional network structure, enhancing the gel's stability and mechanical strength. Polyethylene glycol diacrylate (PEGDA), an unstable crosslinking agent, contains an ester group structure that undergoes hydrolysis under reservoir conditions, conferring biodegradable properties to the gel. Therefore, this study adopts a binary crosslinking system composed of both PEGDA and MBA, in which the ratio between the two crosslinking agents is varied, to achieve the control of degradation time. This crosslinking shell encapsulates PLA particles to prolong degradation. Infrared spectroscopy was employed to characterize the chemical structure of TPA. Thermogravimetric analysis was carried out to evaluate the sample's thermal stability, and a scanning electron microscope and an optical microscope were used to observe the microstructure. The compatibility of TPA with the base slurry, as well as its plugging and pressure-bearing performance were also investigated. The changes in swelling ratio and degradation time of the TPA were studied. Furthermore, the degradation mechanism was revealed through the morphological and structural changes observed in TPA in the degradation process.

2. Experimental

2.1. Materials

Acrylamide (AM), *N*,*N*′-methylenebisacrylamide (MBA), polyethylene glycol diacrylate (PEGDA, stabilized with 100 ppm MEHQ and 300 ppm BHT), 2,2-azobisisobutylamidine dihydrochloride (V_{50}), xanthan gum (XC), ethanol, anhydrous sodium carbonate (Na_2CO_3), and potassium chloride (KCl) were purchased from Shanghai Adamas Reagent Co., Ltd. Polylactic acid (PLA) was provided by Jiecheng Plasticizing Co., Ltd. Low viscosity and high purity polyanionic cellulose (LV-PAC) was purchased from Shanghai Maclin Biochemical Co., Ltd. Deionized water was prepared in the laboratory. Bentonite was purchased from Drilling and Exploration Engineering Co.

2.2. Preparation of temporary plugging agent (TPA)

In this study, TPA was synthesized via free radical polymerization in an aqueous solution. A certain amount of AM was added into a beaker and dissolved in an appropriate volume of deionized water under stirring. Then, the crosslinking agents MBA and PEGDA were added sequentially to the homogenous solution. After complete dissolution of the monomers and the crosslinking agents, a specific amount of PLA was introduced slowly into the mixture, followed by the addition of the initiator V_{50}. When the feeding of materials was completed, the solution was transferred

to a water bath and maintained at 55 °C under a nitrogen atmosphere for 4 h. After that, the final solution was freeze-dried to yield the final TPA. Based on the varying ratios of the two cross-linking agents, the products were designated as AP-1, AP-2, AP-3, AP-4, and AP-5. The specific composition is summarized in Table 1.

2.3. Characterization

The prepared TPA was dried and ground into powders, and then mixed with KBr. The mixture was then pressed into pellets for FTIR analysis using a Nicolet iS5 Fourier transform infrared spectrometer over a scanning range of 4000–400 cm^{-1}.

The thermal stability of TPA was determined using a Mettler TGA2 synchronous thermal analyzer. The samples were evenly spread on the sample pan and tested under nitrogen atmosphere. The heating rate was 10 °C/min and the temperature range was 30–800 °C. The mass changes of the samples were recorded at different temperatures.

The core–shell structure of TPA was observed using a NOVEL N300M optical microscope. Dry AP-1 particles were weighed and fully swollen in deionized water. An appropriate amount of swollen TPA particles was transferred via a dropper onto a glass slide for observation at a suitable magnification (Liu et al., 2024).

The morphology and structure of TPA were characterized using a Phenom Pro X scanning electron microscope (SEM). The fully swollen TPA was sectioned into thin slices, frozen, and then freeze-dried in an FD-1A-50 freeze dryer. Subsequently, the dried samples were mounted on conductive adhesive and subjected to gold sputtering before being transferred to the SEM for observation.

2.4. Rheological and filtration test

Different concentrations of TPA particles were added to bentonite-based slurry prepared in advance (4% bentonite + 0.2% Na_2CO_3). After TPA particles were fully dispersed in the base slurry, the rheological properties of the slurry were measured using a ZNN-D6B electric rotary viscometer at 3, 6, 100, 200, 300, and 600 rpm, recorded as θ_3, θ_6, θ_{100}, θ_{200}, θ_{300}, and θ_{600}, respectively. Then the apparent viscosity (AV), plastic viscosity (PV), and yield point (YP) were calculated. The filtration was then determined with a ZNS-5A medium pressure filter at 25 °C and 0.69 MPa.

2.5. Swelling test

TPA sample, with a mass of m_1, was weighed and added to deionized water, and then placed in a 30 °C water bath. At regular intervals, the surface water was wiped from the particles using filter paper, and the mass m_2 was recorded. This process was repeated until the swelling of TPA reached equilibrium. The swelling ratio was calculated using Eq. (1).

$$S = (m_2 - m_1) / m_1 \quad (1)$$

Table 1
Specific composition of each group of products.

Product No.	AM, wt%	PLA, g	MBA, wt%	PEGDA, wt%	V_{50}, wt%
AP-1	20	8.6	0.45	0.05	0.50
AP-2	20	8.6	0.40	0.10	0.50
AP-3	20	8.6	0.35	0.15	0.50
AP-4	20	8.6	0.30	0.20	0.50
AP-5	20	8.6	0.25	0.25	0.50

where S is the swelling ratio; m_1 is the mass of the TPA before water absorption, g; m_2 is the mass of the TPA after water absorption, g.

2.6. Degradation test

TPA was placed in deionized water and reacted in an oven at different temperatures. Observations were made at intervals of 10 h until the TPA changed from a solid gel to a low-viscosity flowable liquid. The total time required for this change was recorded as the degradation time (Li et al., 2025).

2.7. Sand bed plugging test

The plugging performance of the TPA was tested using the FA-BX portable visual sand bed filtration loss meter, and its plugging ability for sand beds with different mesh sizes was determined at the meantime. TPA particles with different mass concentrations were added to the pre-prepared bentonite-based slurry; after the TPA particles were fully dispersed in the base slurry, the blended slurry was injected into the sand-packed column. The test was carried out under a pressure of 0.69 MPa for 30 min, and the invasion depth of the sand bed was recorded subsequently.

2.8. Pressure-bearing test

A portable high-temperature and high-pressure leak detection device was used to evaluate the pressure-bearing capacity of TPA, and the experimental procedure is specified as follows:

(1) A wedge-shaped fracture with an inlet of 3.0 mm and an outlet of 1.0 mm was selected and placed in the core holder. The confining pressure was set at 20 MPa, and the downstream valve of the core holder was closed. Following the connection of pipelines and sensors, the prepared plugging slurry was injected into the kettle body upstream of the core holder.
(2) The water pump connected to the kettle body was turned on to increase the pressure inside the kettle to 1 MPa. After stabilizing the pressure for 5 min, the downstream valve of the core holder was opened to observe the initial leakage.
(3) The pressure in the kettle was increased continuously at a rate of 1 MPa/5 min, with real-time monitoring of the leakage. A negligible leakage or complete cessation of leakage indicated a favorable plugging effect at the current pressure.
(4) The pressure was further increased continuously until a sudden pressure drop occurred or the leakage volume rose sharply. The maximum pressure achieved before this occurrence was defined as the ultimate pressure-bearing capacity.

2.9. Reservoir protection test

The core displacement apparatus was used to evaluate the reservoir protection performance of TPA. The physical parameters of the cores used are listed in Table 2. The experimental procedure is specified as follows:

(1) The core was placed in the core holder and subjected to confining pressure, and the initial permeability K_1 of the core was measured.

Table 2
Physical parameters of fractured cores.

Core No.	Length, cm	Diameter, cm	Fracture width
1	5.0	2.5	1.0 mm
2	5.0	2.5	Wedge-shaped fracture with an inlet of 3.0 mm and an outlet of 1.0 mm

(2) The plugging slurry was injected under a constant injection pressure. Once the plugging layer was formed, the permeability K_2 was measured.
(3) Subsequently, the core was aged in a 120 °C oven. The permeability K_3 was measured every 12 h until TPA degraded completely.

The plugging rate (R_p) and permeability recovery rate (K_r) were calculated according to Eqs. (2) and (3), respectively.

$$R_p = \frac{K_1 - K_2}{K_1} \times 100\% \quad (2)$$

$$K_r = \frac{K_3}{K_1} \times 100\% \quad (3)$$

where K_1 is the initial permeability of the core, mD; K_2 is the permeability after plugging, mD; K_3 is the permeability after plugging removal, mD.

3. Results and discussion

3.1. Characterizations

3.1.1. FT-IR analysis

The structure of TPA was characterized by FT-IR analysis. FT-IR spectrum of AP-1 is shown in Fig. 1. For comparison, the spectrum of PAM (without PLA) under identical conditions is also shown.

In the spectrum of PLA, the absorption peak at 1723 cm^{-1} is attributed to the stretching vibration of C=O in ester group, while the peak at 1280 cm^{-1} corresponds to the stretching vibration of C–O in ester group.

In the spectrum of PAM, the absorption peak at 3439 cm^{-1} corresponds to $-NH_2$ group in amide bond, while C=O stretching vibration appears at 1635 cm^{-1}. Since the synthetic precursor PEGDA contains ester group, the characteristic absorption peaks for C=O and C–O stretching vibrations of ester group are observed at 1709 and 1315 cm^{-1}, respectively, confirming the successful incorporation of PEGDA.

In the spectrum of AP-1, the following characteristic absorption peaks are listed as below: $-NH_2$ stretching vibration of amide group at 3433 cm^{-1}, C=O stretching vibration of amide group at 1660 cm^{-1}, C=O stretching vibration of ester group at 1723 cm^{-1}, and C–O stretching vibration of ester group at 1298 cm^{-1}. A comparison of the spectra of PAM and AP-1 reveals that no absorption peaks are attributed to C=C bonds, indicating that the reaction between AM and the crosslinking agent occurred via cleavage of C=C bonds. The characteristic absorption peaks corresponding to both PLA and AM in the spectrum of AP-1 confirm that TPA was successfully synthesized.

3.1.2. TGA analysis

As shown in Fig. 2, the thermogravimetric loss of AP-1 is mainly divided into three stages. In the first stage (30–250 °C), the mass change was 9.81% with a slower heating rate, representing the minimum mass loss. This stage is mainly attributed to the loss of free water adsorbed from air and bound water, as well as other volatile substances. In the second stage (250–327 °C), the mass loss was 35.66%. This stage is mainly attributed to the thermal degradation of the amide and ester groups, accompanied by the occurrence of imidization to generate nitriles and long-chain alkanes. In the third stage (327–480 °C), the mass loss was 35.40%. Under high temperatures, the C–C bonds of AP-1 may break and small molecules may be generated.

3.1.3. Optical microscope analysis

As seen in Fig. 3, the structure of PLA and AP-1 was characterized via an optical microscope. In Fig. 3(a), the circular PLA particles are uniformly dispersed in water with a smooth and uncoated surface. Fig. 3(b) reveals that AP-1 particles consist of dark PLA cores and a transparent outer coating layer, presenting the core–shell morphological characteristics. This structure incorporates PLA as the core material, encased in a three-dimensional network structure of PAM; the crosslinked shell layer is used to retard the degradation of the PLA core, thereby enhancing the heat endurance of TPA.

3.1.4. SEM analysis

The microstructure of AP-1 was observed using a field emission scanning electron microscope. As shown in Fig. 4(a), AP-1 features

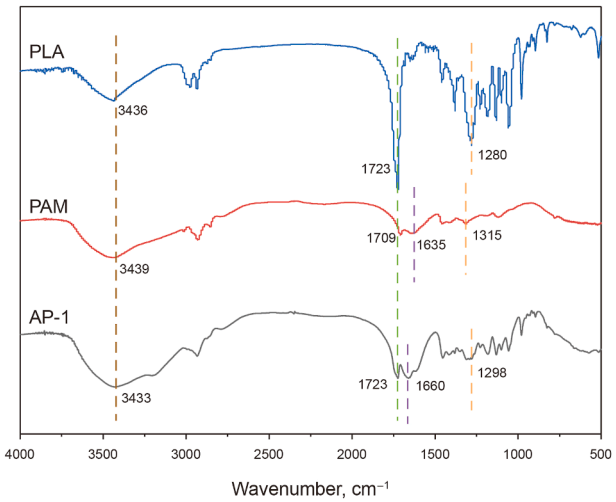

Fig. 1. FT-IR spectra of AP-1, PAM, and PLA.

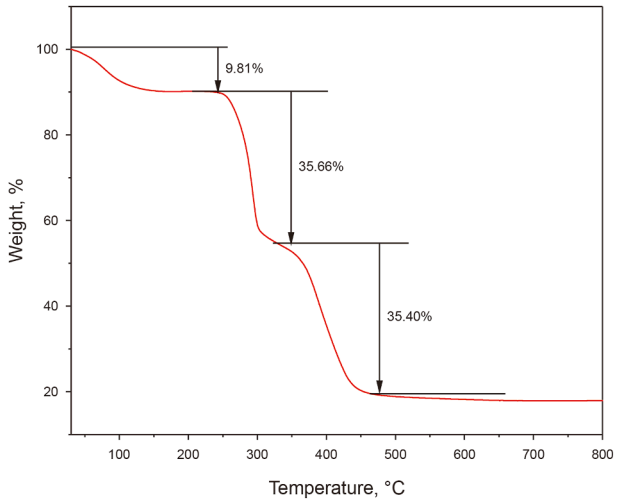

Fig. 2. Thermogravimetric analysis curve of AP-1.

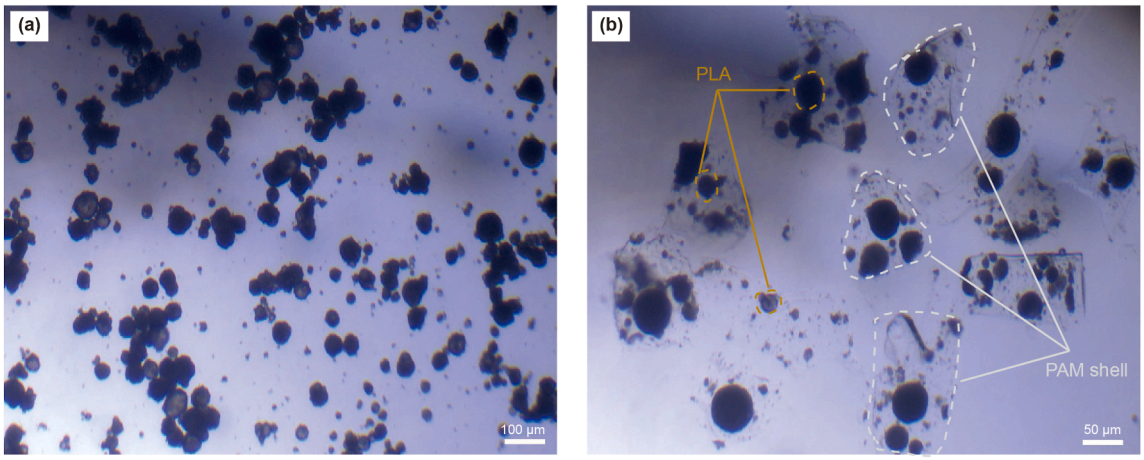

Fig. 3. Microscopic structures: (**a**) PLA, (**b**) AP-1.

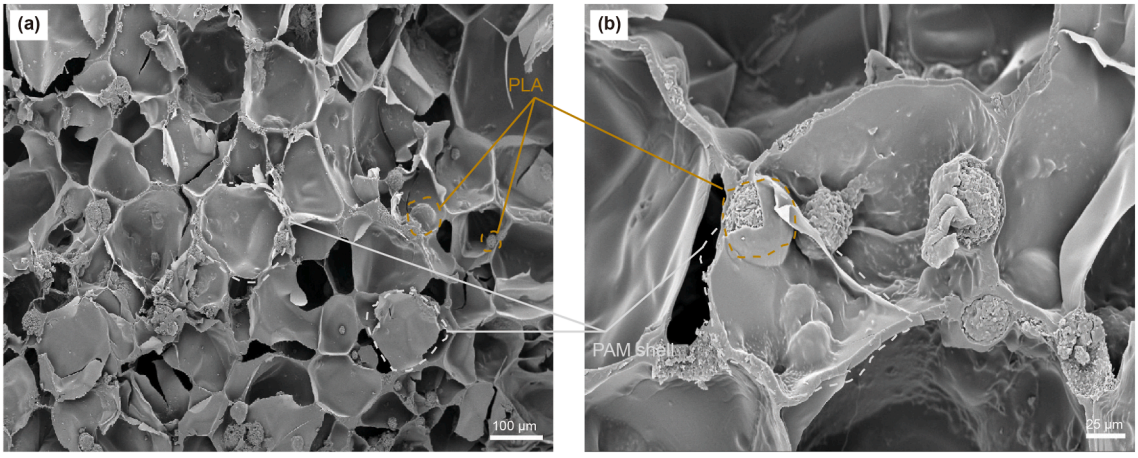

Fig. 4. Microstructure of AP-1.

a relatively complete network structure, with PLA particles embedded in the pores. Fig. 4(b) shows a magnified view of a local region of AP-1. It can be seen that the PLA core is encapsulated by the polyacrylamide shell layer. Structure analysis of AP-1 reveals that during the reaction, free radicals continuously attack acrylamide monomers, initiating chain growth and the formation of linear polyacrylamide segments. The original independent linear polyacrylamide chains are continuously connected by the crosslinking agent. When the crosslinking density reaches a certain level, the originally dispersed and movable linear polymer chains are woven into a continuous network structure via covalent bonds, which endows TPA with a rapid water absorption capacity and certain compressibility.

3.2. Rheological properties and filtration

The effects of AP-1 concentration on the rheological and filtration properties of base slurry were investigated at different aging times and 120 °C. The results are shown in Fig. 5. As the concentration of AP-1 increased, the AV and PV of the system gradually increased, and the filtration gradually decreased. This is because the increase in AP-1 concentration directly raises the solid particle concentration in the system, leading to increased friction and collision probabilities between solid particles and thus raising the flow resistance of the system. In addition, AP-1 exerts a certain binding effect on water, which reduces the free water content in the system. These two factors ultimately result in the increase in both AV and PV. Moreover, the increased solid content improves the compactness of the filter cake, making its structure denser and preventing the liquid phase from passing through, which is reflected in the decrease in filtration.

At room temperature, 0.5% AP-1 reduced the filtration of base slurry from 30 to 19 mL. After aging, the base slurry with AP-1 also exhibited better filtration control. Within the first 2 h of aging, AV, PV, YP, and FL_{API} did not change significantly, indicating that AP-1 does not affect the rheological properties during the pumping process. However, after 16 h, AV, PV, and YP increased significantly. AP-1 continuously absorbed water, resulting in a decrease in free water and an increase in viscosity. At this stage, the mismatch between the particle size of AP-1 and the pore size of filter paper has a less effect on filtration reduction compared to the decrease in free water in the slurry, resulting in reduced filtration. This also demonstrates that AP-1 can maintain structural integrity at 120 °C and still exist in base slurry (Bai et al., 2023).

3.3. Swelling analysis

The water absorption properties of products composed of different crosslinking agents are presented in Fig. 6. All products exhibited rapid water absorption within the first 10 min, with the swelling ratio rising sharply. The water absorption reached

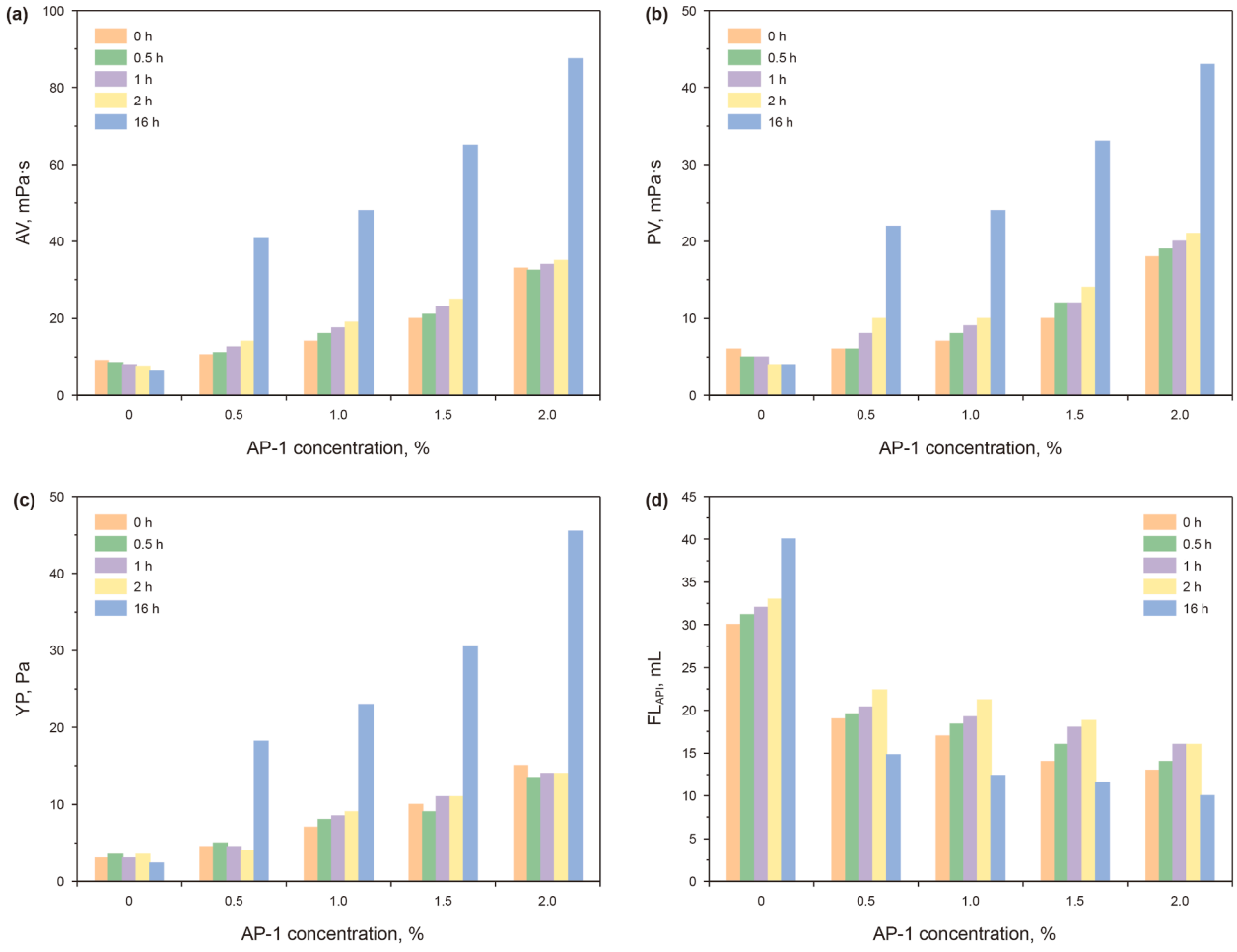

Fig. 5. Effect of AP-1 concentration on rheological properties and filtration of the drilling fluid before and after aging at 120 °C: (**a**) AV, (**b**) PV, (**c**) YP, (**d**) FL_{API}.

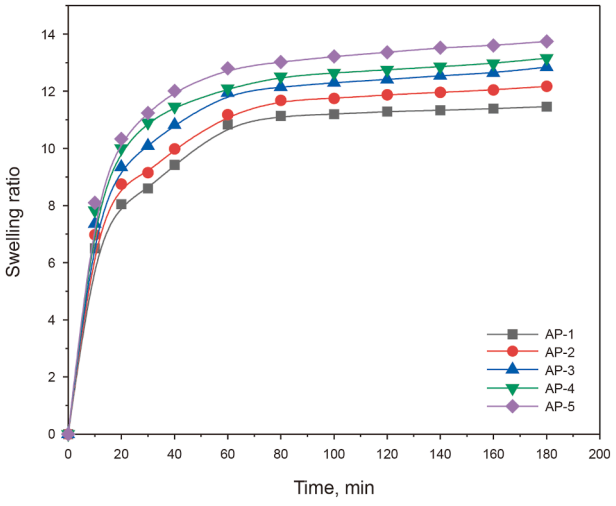

Fig. 6. Effect of different crosslinking agent compositions on swelling ratio.

equilibrium at 60 min, and no significant changes were observed thereafter. As the proportion of PEGDA in the crosslinking agent increased, the maximum swelling ratio increased from 11.46 to 13.74.

The increase in swelling ratio can be attributed to the polyethylene glycol segments in PEGDA. The hydrophilicity of polyethylene glycol enhances the hydration effect, which increases the number of hydrophilic sites in the molecular chain and enhances the water absorption capacity. Furthermore, MBA is a bifunctional small molecule crosslinking agent with a short double bond spacing, which leads to densely distributed crosslinking points and a relatively compact crosslinking network. In contrast, PEGDA has a higher molecular weight and wider double bond spacing. Its long chain structure reduces the crosslinking density and forms a looser crosslinking network. Hence, as the PEGDA proportion increases, the entire crosslinked network structure becomes sparse, allowing it to absorb more water and increase the swelling ratio.

3.4. Plugging evaluation

Quartz sand with different mesh sizes was employed to simulate geological fractures, and AP-1 was selected to investigate the plugging performance on quartz sand beds at different concentrations, with the results are presented in Fig. 7.

In the 40–70 mesh sand bed, the base slurry permeated at a relatively fast speed under 0.69 MPa, fully invading the sand bed within 30 s, and reached an invasion depth of 13 cm. At the AP-1 concentration of 0.5%, the sand bed invasion depth can be greatly reduced. This phenomenon indicates that AP-1 can form an effective plugging layer on the sand bed surface, which can block the invasion of external fluids and thus exert a good plugging effect. In the 70–120 mesh sand bed, a denser crack structure was

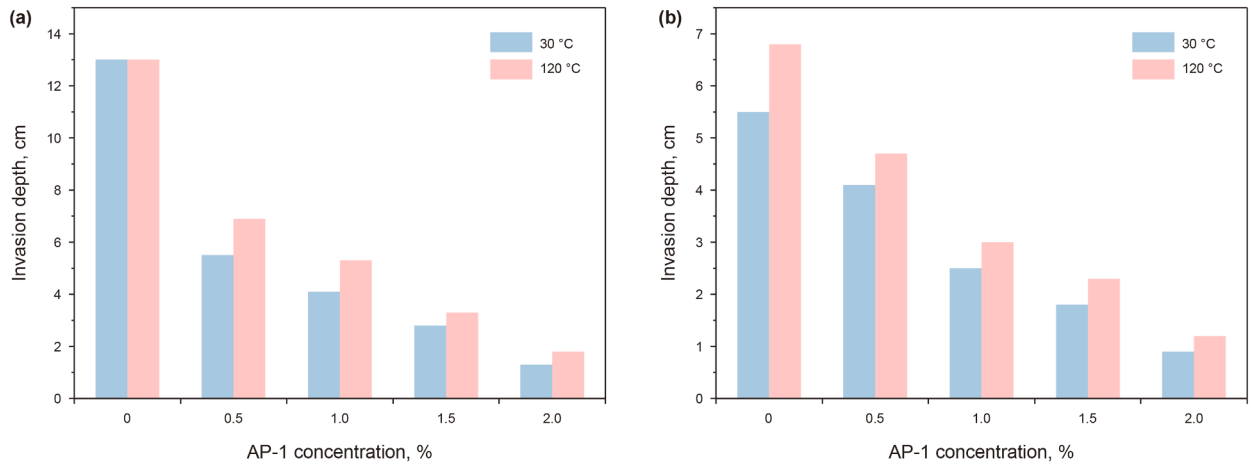

Fig. 7. Effect of AP-1 concentration on sand bed invasion depth: (**a**) 40–70 mesh sand bed, (**b**) 70–120 mesh sand bed.

formed as the grain size of the sand decreases. The invasion depth of the base slurry was 5.5 cm, which correspondingly decreased with increasing AP-1 concentration. As the plugging slurry is injected into the sand bed, AP-1 can further penetrate into the sand bed pores, and AP-1 particles squeeze against each other to form a plugging layer. The particles in the subsequent plugging slurry gradually accumulated on the sand bed surface, preventing the liquid from penetrating deep into the fractures and making the plugging more thorough. When the amount of AP-1 increased, the increase in particles involved in plugging made the formed plugging zone denser. Thus, the invasion depth of sand bed continued to decrease.

To evaluate the plugging performance of AP-1 under high-temperature conditions, the base slurry containing AP-1 was aged at 120 °C for 2 h, following the methodology of Zhai et al. (2020). The plugging test revealed that the invasion depth increased with temperature. This can be attributed to the reduced strength of AP-1 after water absorption and its volumetric expansion, which is insufficient to match the pore throat size. AP-1 can only bridge and accumulate on sand bed surface without penetrating the pores. Nonetheless, the results indicate that AP-1 still remains effective plugging performance even at high temperatures.

A comparison of the plugging performance of AP-1 for different mesh sand beds revealed that its effectiveness decreased as the sand size increased. Consequently, the difficulty of plugging rose with the increase in fracture width. AP-1 had a good ability to plug the sand beds of varied mesh sizes.

3.5. Pressure-bearing evaluation

When plugging larger leakage channels, the sole use of rigid particles can achieve a certain degree of bridging, yet it is difficult to form a high strength and dense plugging layer. In order to form a strong and dense plugging layer, deformable AP-1 particles were used in combination with rigid calcium carbonate particles. Under high pressure, the deformable AP-1 particles fill the voids between rigid particles (Zhong et al., 2022). The wedge-shaped fracture with an inlet of 3.0 mm and an outlet of 1.0 mm was selected for the test. The breakthrough pressure was determined using a stepwise pressure increase method. The experimental results are illustrated in Fig. 8.

In the initial stage, the water pump was turned on to raise the pressure inside the kettle. Once the pressure rose to a certain value, the pressure was stabilized for a certain time. Subsequently, the downstream valve was opened, enabling the plugging slurry to be pressed into the fracture, forming a plugging layer under pressure. Before the valve was opened, the device was in a closed and high-pressure state. After the valve was opened, the device was instantly connected to the atmosphere, resulting in a pressure release similar to balloon deflation and thus a subsequent pressure

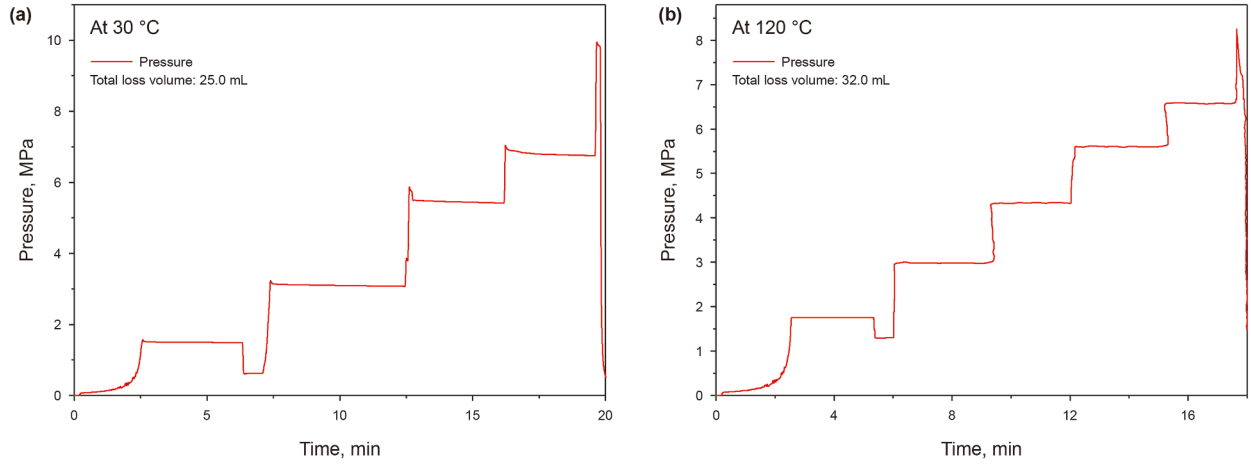

Fig. 8. Pressure curve: (**a**) 30 °C, (**b**) 120 °C.

drop. The pressure then increased incrementally to test the pressure-bearing limit of the plugging layer. The stable pressure-bearing capacity of the plugging layer reached 6.75 MPa at 30 °C and 6.49 MPa at 120 °C, and the total leakage volume was 25.0 and 32.0 mL, respectively. The pressure-bearing capacity only slightly decreased under higher temperature, which demonstrates that AP-1 has excellent plugging and pressure-bearing capacity at 120 °C, and the composite plugging material can effectively plug the wedge-shaped fracture with an inlet of 3.0 mm and an outlet of 1.0 mm.

3.6. Reservoir protection performance evaluation

Experiments were conducted using two fractures and different plugging materials (Jia et al., 2020), with the results presented in Fig. 9 and Table 3. It can be seen from the permeability change curve that AP-1 particles swelled in the early stage, and the permeability change was not obvious. After that, its degradation accelerated and the permeability increased rapidly. In the experiment with AP-1, the permeability recovery rate reached 95.31%. When bridging materials ($CaCO_3$) were also used, the permeability recovery rate exceeded 85%. On the one hand, AP-1 can achieve effective degradation, and on the other hand, the small bridging particles can flow back, while large particles exert a supporting effect in the fracture to prevent fracture closure and maintain conductivity (Guo et al., 2025). The results demonstrate that AP-1 can effectively degrade, exerting less harm to the core, and exhibits excellent reservoir protection performance.

3.7. Degradation behavior and performance evaluation

3.7.1. Effect of temperature on degradation time

To investigate the effect of temperature on degradation time, AP-1 was selected to determine its degradation time at different

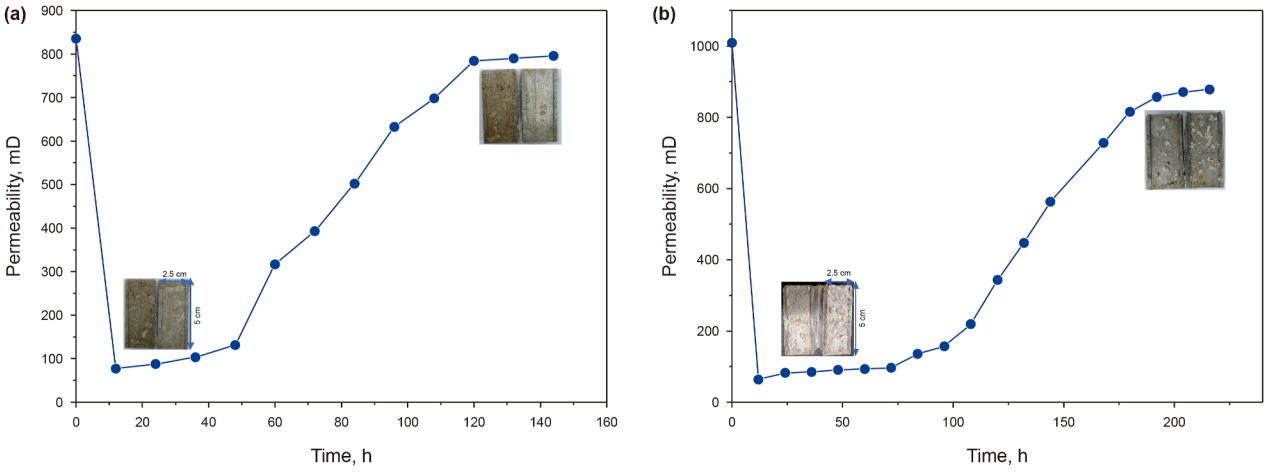

Fig. 9. Permeability curve: (**a**) AP-1, (**b**) AP-1 + $CaCO_3$.

Table 3
Permeability recovery tests.

Core No.	Plugging material	Permeability, mD			Plugging rate, %	Permeability recovery rate, %
		K_1	K_2	K_3		
1	AP-1	835.335	77.205	796.178	90.76	95.31
2	AP-1 + $CaCO_3$	1009.018	14.220	878.542	98.59	87.07

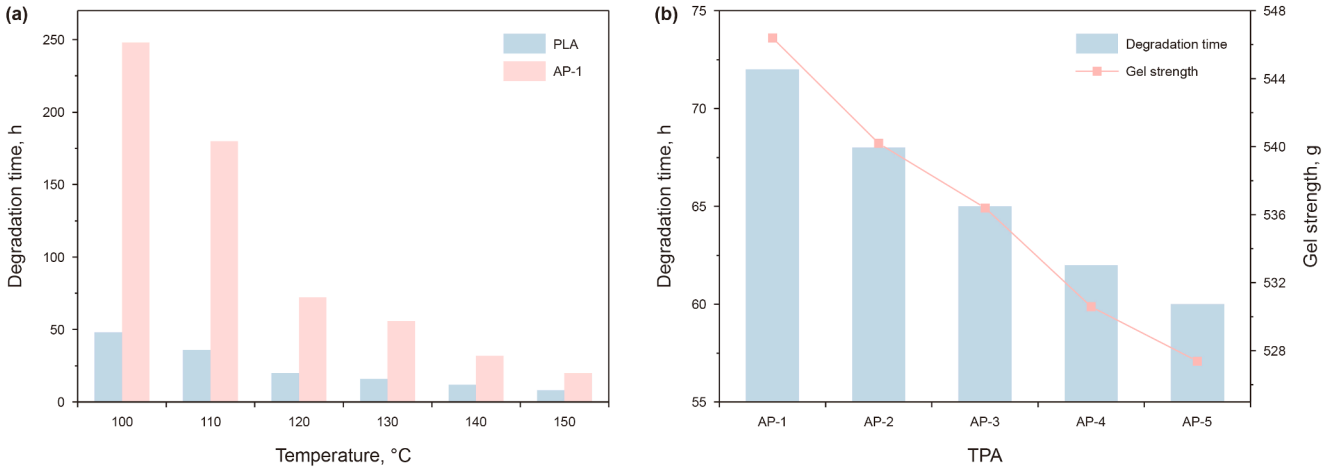

Fig. 10. (**a**) Effect of temperature on degradation time, (**b**) degradation time of TPAs at 120 °C.

temperatures and compared with the degradation of polylactic acid. The results are presented in Fig. 10(a).

The degradation time of AP-1 at 100 °C was 248 h, which was 200 h longer than that of PLA. Heating effectively activates the movement of PLA molecular chain segments. At this state, PLA particles enter a viscous flow state, where water molecules easily penetrate, and accelerate the degradation. However, AP-1 has a three-dimensional network, which shows a slower degradation process. When the temperature rose to 150 °C, the degradation time of both AP-1 and PLA decreased significantly, with 20 h for AP-1 and 8 h for PLA. The thermal motion of water molecules becomes more intense, accelerating the hydrolysis reaction rate of ester and amide groups in the molecular structures of PLA and AP-1 (Xu et al., 2024). It causes the cleavage of molecular chains in PLA and AP-1 structures (Xiong et al., 2018), contributing to increased degradation rate.

In summary, the degradation rate exhibits a positive correlation with temperature. As the temperature increases, the thermal motion of water molecules intensifies, and thus effectively accelerates the hydrolysis of weak chemical bonds, resulting in an increase in the degradation rate.

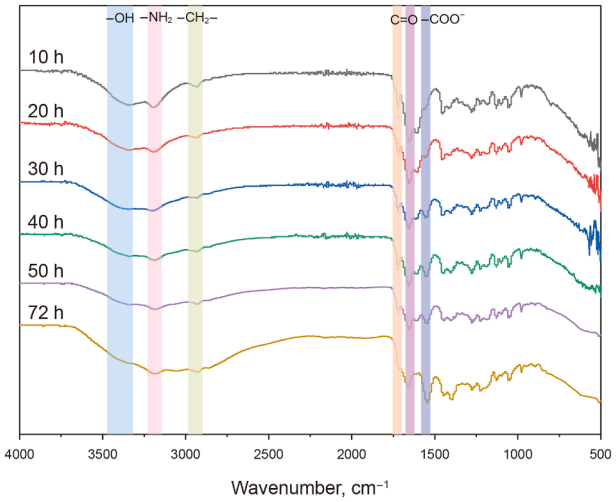

Fig. 11. Structural changes of AP-1 during degradation.

3.7.2. *Effect of crosslinking agent ratio on degradation time*

The degradation time of products with crosslinker was measured at 120 °C, and the gel strength was determined using a Brookfield CT3 texture analyzer. The results are presented in Fig. 10(b). The degradation time of AP-1 exhibited a linear correlation with PEGDA proportion. As the PEGDA proportion increased, the degradation time of AP-1 was reduced accordingly. When the PEGDA proportion increased from 10% to 50%, the degradation time was reduced from 72 to 60 h, indicating that the degradation time can be adjusted by changing PEGDA percentage in crosslinking agents to meet engineering requirements.

The change in degradation time is closely related to the change in the internal crosslinking network. When the proportion of PEGDA increases, the ester group content in AP-1 rises, and the crosslinking structure transforms from dense to loose. This structural evolution does harm to the stability of the network and makes the latter easier to degrade.

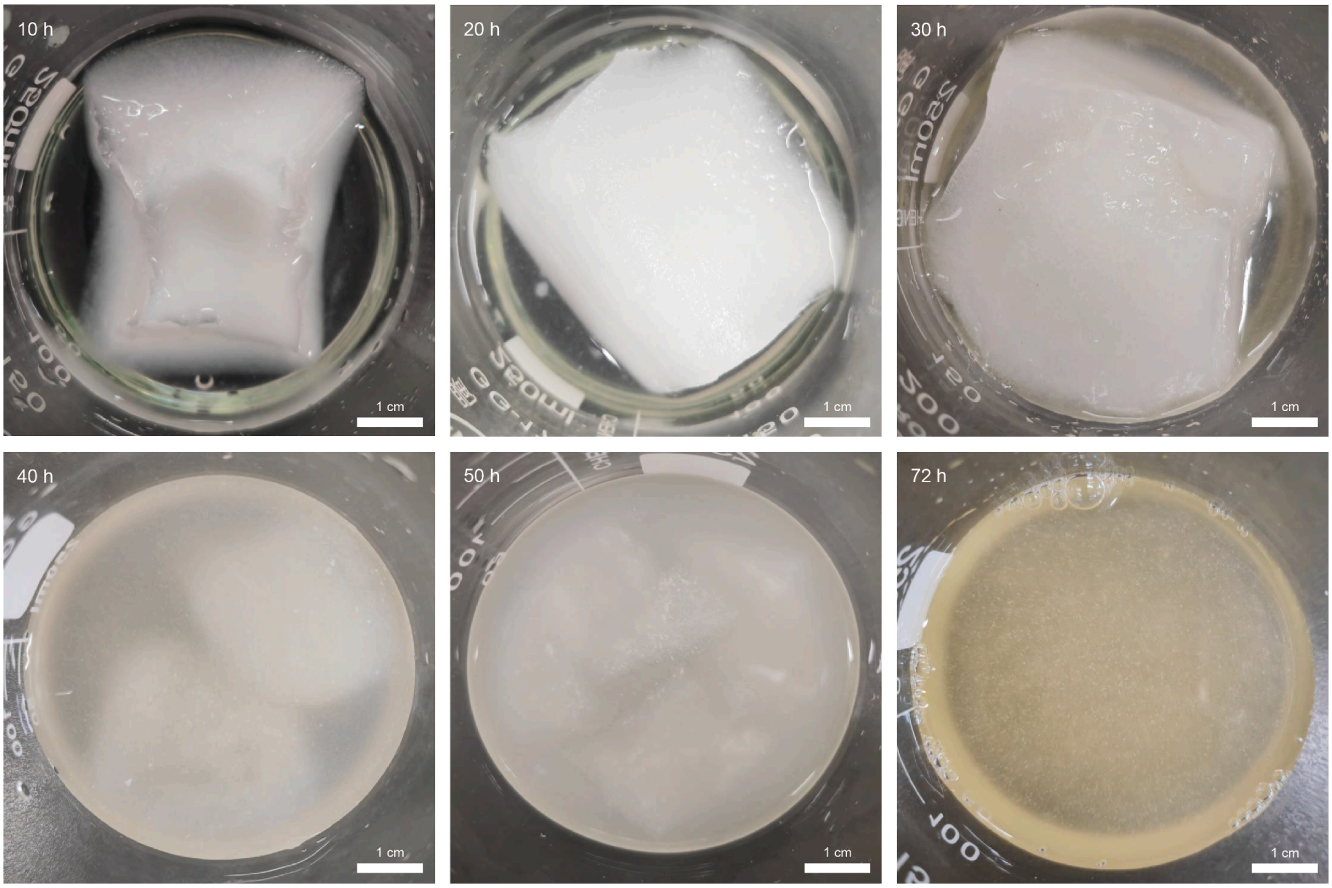

Fig. 12. Morphological changes of AP-1 during degradation.

3.7.3. Structural changes in the degradation process

Fig. 11 shows the infrared spectra of degraded AP-1 at different degradation stages. The absorption peaks appear to be roughly unchanged. The peak at 2930 cm^{-1} corresponds to the asymmetric stretching vibration of methylene –CH_2–, the peak at 1730 cm^{-1} corresponds to the C=O stretching vibration in ester group, and the peak at 1640 cm^{-1} corresponds to C=O absorption peak in amide group. As degradation proceeded, the absorption peak corresponding to ester group gradually decreased, due to the cleavage of the functional group. This phenomenon signifies the disappearance of crosslinking points formed by PEGDA, leading to the disintegration of gel network and the continuous degradation of internal PLA. The degradation of amide groups causes a slight weakening of the –CH_2– absorption peak, while the absorption peak corresponding to –COO^- (1540 cm^{-1}) gradually increased. This indicates that amide groups undergo hydrolysis to form carboxylic acid groups in aqueous solution (Luo et al., 2023). A broad absorption peak appeared at approximately 3400 cm^{-1}, which is attributed to carboxylic acid groups, alcohols, and carboxylic acids generated by amide hydrolysis (Ma et al., 2015; Zhang et al., 2023). The analysis above demonstrates that AP-1 degradation is mainly caused by the cleavage of amide and ester groups.

3.7.4. Morphological changes in the degradation process

In order to study the macroscopic and microscopic morphological changes of AP-1 during the degradation process, a combination of macroscopic and microscopic characterization methods was adopted to observe the morphology under 120 °C. The hydrophilic groups and three-dimensional network structure endow AP-1 with water absorption and swelling capabilities. In the initial stage, AP-1 gradually absorbed water and swelled, leading to an increase in volume and mass. Once water absorption reached saturation, AP-1 began to degrade under the sustained influence of temperature.

As shown in Figs. 12 and 13, the degradation process of AP-1 presents stage-wise characteristics. After 10 h of degradation, AP-1 retained a complete structure with well-defined edges and corners. At this stage, the high-temperature environment promoted the movement of small molecules, with a large percentage of water molecules penetrating into AP-1 and causing swelling and expansion. After 20 h of degradation, AP-1 exhibited no obvious change but showed a slight decrease in strength. Partial crosslinking sites fractured, resulting in an irregular network structure. After 30 h of degradation, the edges of AP-1 began to disappear and its strength declined further, but it still maintained a relatively intact macroscopic morphology. Its microscopic morphology showed a complex porous network structure. Due to the disappearance of the crosslinking sites, some holes collapsed, and the exposed PLA particles initiated degradation. After 40 h of degradation, obvious cracks appeared on AP-1, the degradation solution became turbid, and some degradation products formed a white film at the bottom of the container. The microstructure showed flake-like structures with varying sizes, overlapping and wrinkling features, and PLA particles were visible on the surface. After 50 h of degradation, AP-1 disintegrated into smaller fragments with the shell layer basically degraded. The released PLA particles aggregated at the bottom of the container, and the microstructure was porous and irregularly flaky, which was caused by molecular chain

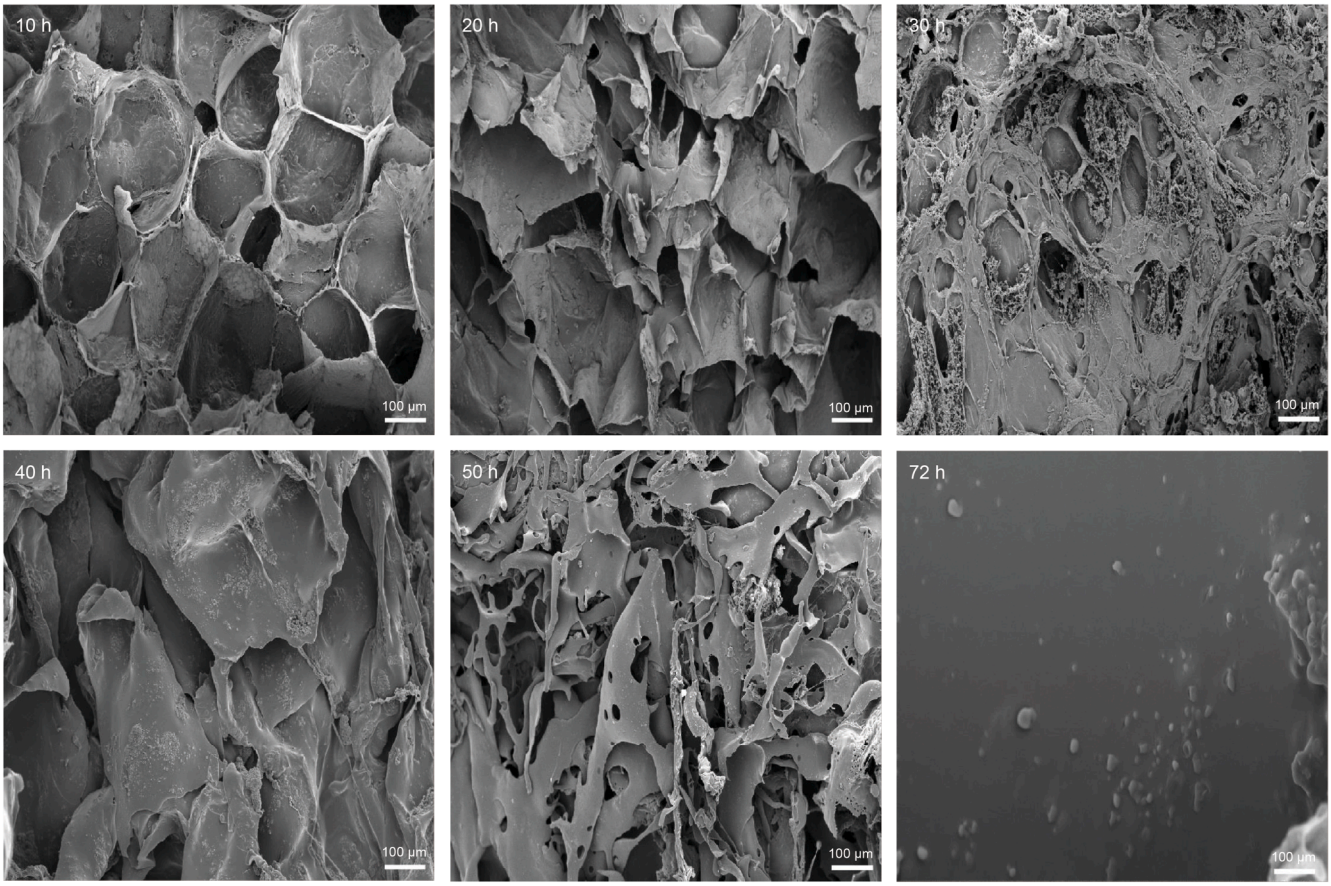

Fig. 13. Microstructural changes of AP-1 during degradation.

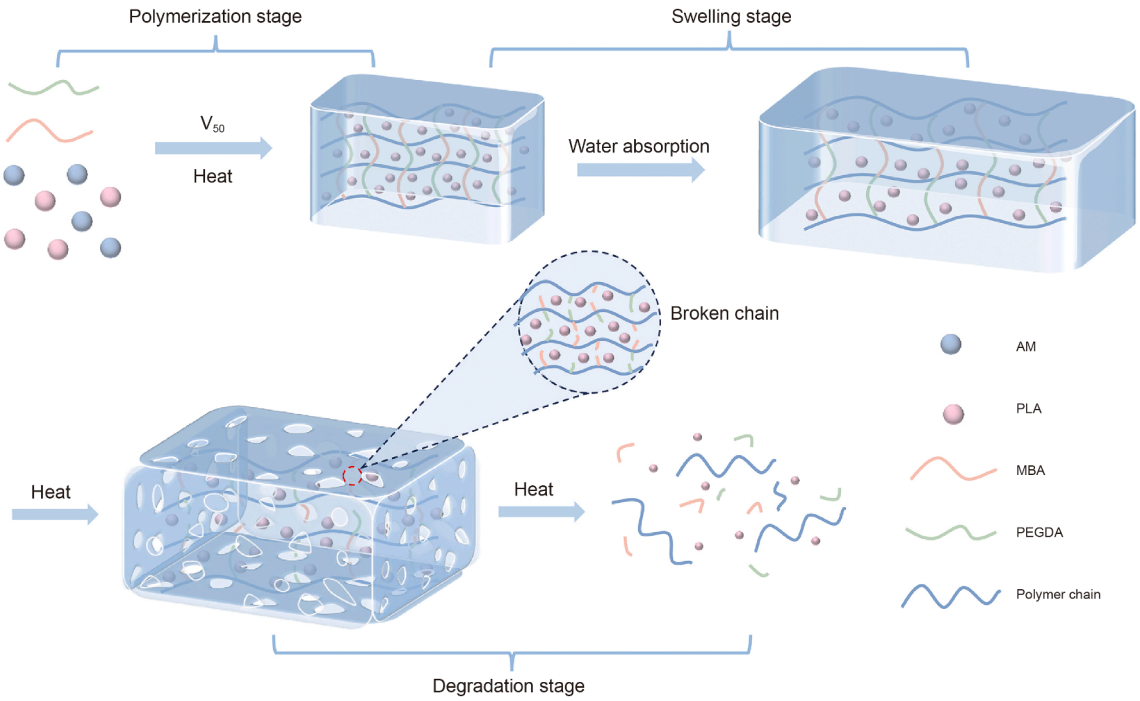

Fig. 14. Synthesis, swelling, and degradation of AP-1.

cleavage and structure disintegration during the degradation process. In the final stage, the remaining substances were degraded into water-soluble small-molecule monomers, and no visible network structure remained at the microscopic level. Ultimately, AP-1 degraded into a light yellow, low-viscosity solution.

3.8. Mechanism of synthesis and self-degradation of AP-1

The synthesis and self-degradation mechanisms of AP-1 are illustrated in Fig. 14. During the synthesis, under the synergistic effect of crosslinking agent MBA and PEGDA, acrylamide monomers form a three-dimensional network structure through free radical polymerization reaction, with the PLA particles encapsulated as the core. The hydrophilic groups in AP-1, together with the three-dimensional network structure, endow it with the ability to absorb water and swell. During the degradation, sustained heating renders AP-1 shell porous and exposes part of the PLA. Water molecules penetrate into the interior and continuously interact with PLA, causing the cleavage of amide and ester groups. This leads to the gradual disappearance of crosslinking points, the progressive disintegration of the three-dimensional network structure, and the formation of a folded flake structure. Subsequently, the structure gradually degrades into irregular linear chains, which are no longer capable of encapsulating PLA as the core. The exposed PLA undergoes further degradation and completely breaks down.

4. Conclusions

In this study, a self-degradable temporary plugging agent (TPA) was prepared via free radical polymerization in aqueous solution. Its chemical structure and thermal stability were characterized by infrared and thermogravimetric analysis, and its core–shell structure was confirmed by optical microscopy and scanning electron microscopy. The rheological properties, filtration, plugging and pressure-bearing performance, and degradation of TPA (AP-1) were tested. The findings are as follows:

(1) AP-1 has little impact on the rheological properties of base slurry, exhibiting excellent compatibility with base slurry and enabling effective reduction of filtration. When 0.5% AP-1 was used, mud filtration can be reduced by 11 mL.
(2) Sand bed plugging experiments showed that AP-1 forms an effective plugging layer on the sand bed surface. For 40–70 mesh sand bed, it reduced the invasion depth from 13 to 1.3 cm, while it reduced the invasion depth from 5.5 to 0.9 cm for 70–120 mesh sand bed.
(3) The pressure-bearing experiment indicated that the synergistic effect of using AP-1 as filler particles in collaboration with rigid bridging particles ($CaCO_3$). This collaboration enabled the plugging system to achieve a pressure-bearing capacity of 6.75 MPa.
(4) By adjusting the proportion of crosslinking agent, the swelling ratio of TPA can be increased from 11.46 to 13.74, and its degradation time can be regulated within the range of 60–72 h. The degradation mechanism was speculated, mainly due to the cleavage of amide and ester groups.

In summary, the introduction of unstable crosslinking points into TPA structure enables self-degradation under high temperatures, resulting in minimal reservoir damage. Additionally, the degradation duration of TPA can be adjusted through the design of the synthetic formulation.

CRediT authorship contribution statement

Jia-Rui Li: Writing – original draft, Investigation, Data curation. **Ling Lin:** Writing – review & editing, Funding acquisition, Conceptualization. **Lei Li:** Project administration, Investigation. **Hao Lu:** Supervision, Formal analysis, Conceptualization. **Cheng-**

Yuan Xu: Resources, Project administration. **Xin-Min Zhang:** Validation, Supervision. **Wen Ren:** Visualization, Project administration.

Declaration of interest statement

No competing interest exits in the submission of this manuscript, and manuscript is approved by all authors for publication. The work described is original research that has not been published previously, and not under consideration for publication elsewhere, in a whole or in part. All the authors listed have approved the manuscript that is enclosed.

Acknowledgements

This work was supported by The Opening Project of Oil & Gas Field Applied Chemistry Key Laboratory of Sichuan Province (Grant number YQKF202214).

References

Bai, X.D., Wang, M.B., Chen, Y., et al., 2023. Synthesis and properties of self-healing hydrogel plugging agent. J. Appl. Polym. Sci. 141. https://doi.org/10.1002/app.55005.

Bai, Y.R., Dai, L.Y., Sun, J.S., et al., 2022a. Plugging performance and mechanism of an oil-absorbing gel for lost circulation control while drilling in fractured formations. Pet. Sci. 19, 2941–2958. https://doi.org/10.1016/j.petsci.2022.08.004.

Bai, Y.R., Liu, C.T., Sun, J.S., et al., 2022b. High temperature resistant polymer gel as lost circulation material for fractured formation during drilling. Colloids Surf. A Physicochem. Eng. Asp. 637, 128244. https://doi.org/10.1016/j.colsurfa.2021.128244.

Chen, X., Lu, X., Liu, P.L., et al., 2024. A critical review of key points in temporary plugging fracturing: Materials, injection, temporary plugging, and design. Geoenergy Sci. Eng. 240, 212981. https://doi.org/10.1016/j.geoen.2024.212981.

Chen, Z.R., Wu, G.G., Zhou, J., et al., 2023. Optimization of degradable temporary plugging material and experimental study on stability of temporary plugging layer. Front. Phys. 11, 1167215. https://doi.org/10.3389/fphy.2023.1167215.

Cui, K.X., Jiang, G.C., Yang, L.L., et al., 2021. Preparation and properties of magnesium oxysulfate cement and its application as lost circulation materials. Pet. Sci. 18, 1492–1506. https://doi.org/10.1016/j.petsci.2021.08.002.

Dindoruk, B., Zhang, F.Y., 2024. Advances in drilling and completion fluid technologies for protecting oil and gas reservoirs: Research progress and development trends. J. Energy Res. Technol. Transac. Asme 146, 50801. https://doi.org/10.1115/1.4064472.

Elsawy, M.A., Kim, K.H., Park, J.W., et al., 2017. Hydrolytic degradation of polylactic acid (PLA) and its composites. Renem. Sustain. Energy Rev. 79, 1346–1352. https://doi.org/10.1016/j.rser.2017.05.143.

Gong, W.Z., Huang, W.A., Liu, J., et al., 2021. Synthesis, characterization, and performance evaluation of starch-based degradable temporary plugging agent for environmentally friendly drilling fluid. Lithosphere 2021, 14. https://doi.org/10.2113/2021/6679756.

Guo, K., Kang, Y.L., Xu, C.Y., et al., 2025. A quantitative evaluation method for lost circulation materials in bridging plugging technology for deep fractured reservoirs. SPE J. 30 (8), 4706–4725. https://doi.org/10.2118/228302-PA.

Guo, P., Tian, Z.K., Zhou, R., et al., 2022. Chemical water shutoff agents and their plugging mechanism for gas reservoirs: A review and prospects. J. Nat. Gas Sci. Eng. 104, 104658. https://doi.org/10.1016/j.jngse.2022.104658.

Jia, H., Yang, X.Y., Li, S.X., et al., 2020. Nanocomposite gel of high-strength and degradability for temporary plugging in ultralow-pressure fracture reservoirs. Colloids Surf. A Physicochem. Eng. Asp. 585, 124108. https://doi.org/10.1016/j.colsurfa.2019.124108.

Kang, S.F., Pu, C.S., Wang, K., et al., 2023. Investigation of the oil-soluble particulate temporary plugging agent-assisted water huff'n'puff enhanced oil recovery in tight oil reservoirs. SPE J. 28 (5), 2346–2364. https://doi.org/10.2118/215855-PA.

Li, J., Wu, D.P., Zhang, R., et al., 2023. Evaluation method for reservoir damage of cementing slurry. Front. Energy Res. 11, 1227981. https://doi.org/10.3389/fenrg.2023.1227981.

Li, M., Gong, W.H., Wang, F., et al., 2025. A novel carbon dot-based degradable preformed particle gel for sensitive detection of iron ions. Colloids Surf. A Physicochem. Eng. Asp. 711, 136414. https://doi.org/10.1016/j.colsurfa.2025.136414.

Liu, C., Zou, H.J., Wang, Y.G., et al., 2024. Degradation behavior and mechanism of P(AM/AA/AMPS)@PLA core-shell self-degrading temporary plugging agent. J. Mol. Liq. 393, 123656. https://doi.org/10.1016/j.molliq.2023.123656.

Liu, H.B., Li, X.M., Pan, Z., et al., 2025. Lignin-based plugging hydrogel with high-temperature resistance and adjustable gelation. Adv. Compos. Hybrid Mater. 8, 111. https://doi.org/10.1007/s42114-024-01132-w.

Liu, J.P., Fu, H.R., Luo, Z.F., et al., 2023. Preparation and performance of pH-temperature responsive low-damage gel temporary plugging agent. Colloids Surf. A Physicochem. Eng. Asp. 662, 130990. https://doi.org/10.1016/j.colsurfa.2023.130990.

Liu, S., Guo, T.K., Rui, Z.H., et al., 2020. Performance evaluation of degradable temporary plugging agent in laboratory experiment. J. Energy Res. Technol. 142, 123002. https://doi.org/10.1115/1.4047311.

Luo, Y.H., Lin, L., Guo, Y.J., et al., 2023. Study on high-temperature degradation of acrylamide-based polymer ZP1 in aqueous solution. Polym. Degrad. Stabil. 217, 110533. https://doi.org/10.1016/j.polymdegradstab.2023.110533.

Ma, Q.S., Shuler, P.J., Aften, C.W., et al., 2015. Theoretical studies of hydrolysis and stability of polyacrylamide polymers. Polym. Degrad. Stabil. 121, 69–77. https://doi.org/10.1016/j.polymdegradstab.2015.08.012.

Sun, J.S., Bai, Y.R., Cheng, R.C., et al., 2021. Research progress and prospect of plugging technologies for fractured formation with severe lost circulation. Petrol. Explor. Dev. 48, 732–743. https://doi.org/10.1016/S1876-3804(21)60059-9.

Tang, X.L., Duan, W.M., Yang, M., et al., 2023. Construction and degradation mechanism of polylactic acid-pH-responsive microgel composite system plugging system. J. Dispersion Sci. Technol. 44, 2532–2540. https://doi.org/10.1080/01932691.2022.2106996.

Wang, G., He, S.Y., Yu, J.M., et al., 2024. In-situ poly (hexahydrotriazine) gels temporary plugging agent suitable for high-temperature reservoirs: Regulation by inorganic chloride salts. Geoenergy Sci. Eng. 239. https://doi.org/10.1016/j.geoen.2024.212905.

Wang, Y., Liu, D.J., Liao, R.Q., et al., 2022. Study of adhesive self-degrading gel for wellbore sealing. Colloids Surf. A Physicochem. Eng. Asp. 651, 129567. https://doi.org/10.1016/j.colsurfa.2022.129567.

Wu, G.G., Chen, Z.R., Zhang, A.S., et al., 2023. Experimental studies on the performance evaluation of water-soluble polymers used as temporary plugging agents. Front. Phys. 11, 1174268. https://doi.org/10.3389/fphy.2023.1174268.

Xiong, C.M., Wei, F.L., Li, W.T., et al., 2018. Mechanism of polyacrylamide hydrogel instability on high-temperature conditions. ACS Omega 3, 10716–10724. https://doi.org/10.1021/acsomega.8b01205.

Xu, C.Y., Xie, J., Kang, Y.L., et al., 2024. Fracture prepropping and temporary plugging for formation damage control in deep naturally fractured tight reservoirs. SPE J. 29, 4737–4752. https://doi.org/10.2118/221489-PA.

Xu, H.L., Zhang, L.J., Wang, J., et al., 2023. Evaluation of self-degradation and plugging performance of temperature-controlled degradable polymer temporary plugging agent. Polymers 15, 3732. https://doi.org/10.3390/polym15183732.

Yang, F., Liu, J.H., Ji, R.J., et al., 2024. Degradable gel for temporary plugging in high temperature reservoir and its properties. Gels 10, 445. https://doi.org/10.3390/gels10070445.

Yang, H.B., Lv, Z.Q., Li, Z., et al., 2023. Laboratory evaluation of a controllable self-degradable temporary plugging agent in fractured reservoir. Phys. Fluids 35, 83314. https://doi.org/10.1063/5.0157272.

Yu, B.W., Zhao, S.D., Long, Y.F., et al., 2022. Comprehensive evaluation of a high-temperature resistant re-crosslinkable preformed particle gel for water management. Fuel 309. https://doi.org/10.1016/j.fuel.2021.122086.

Zaaba, N.F., Jaafar, M., 2020. A review on degradation mechanisms of polylactic acid: Hydrolytic, photodegradative, microbial, and enzymatic degradation. Polym. Eng. Sci. 60, 2061–2075. https://doi.org/10.1002/pen.25511.

Zhai, K.L., Yi, H., Liu, Y., et al., 2020. Experimental evaluation of the shielded temporary plugging system composed of calcium carbonate and acid-soluble preformed particle gels (ASPPG) for petroleum drilling. Energy Fuels 34, 14023–14033. https://doi.org/10.1021/acs.energyfuels.0c02810.

Zhang, G.C., Ran, Y.L., Jiang, P., et al., 2023. A study on the thermal degradation of an acrylamide and 2-acrylamido-2-methylpropanesulfonic acid copolymer at high temperatures. Polymers 15, 2665. https://doi.org/10.3390/polym15122665.

Zhang, H.J., Zhu, D.Y., Gong, Y.L., et al., 2022. Degradable preformed particle gel as temporary plugging agent for low-temperature unconventional petroleum reservoirs: Effect of molecular weight of the cross-linking agent. Pet. Sci. 19, 3182–3193. https://doi.org/10.1016/j.petsci.2022.07.013.

Zhao, L.Q., Chen, X., Zou, H.L., et al., 2020. A review of diverting agents for reservoir stimulation. J. Petrol. Sci. Eng. 187, 106734. https://doi.org/10.1016/j.petrol.2019.106734.

Zhao, X., Zheng, Z., Chen, J.Z., et al., 2024. In-situ experimental study on the hydrolysis and pyrolysis processes of polylactic acid. Polym. Eng. Sci. 64, 1675–1685. https://doi.org/10.1002/pen.26647.

Zhao, Z., Sun, J.S., Liu, F., et al., 2023. Micro-nano polymer microspheres as a plugging agent in oil-based drilling fluid. Colloids Surf. A Physicochem. Eng. Asp. 673, 131808. https://doi.org/10.1016/j.colsurfa.2023.131808.

Zhong, Y., Zhang, H., Feng, Y.H., et al., 2022. A composite temporary plugging technology for hydraulic fracture diverting treatment in gas shales: Using degradable particle/powder gels (DPGs) and proppants as temporary plugging agents. J. Pet. Sci. Eng. 216, 110851. https://doi.org/10.1016/j.petrol.2022.110851.

Zhou, Q., Luo, Z.F., Fu, H.R., et al., 2025. Research and application progress of temporary plugging agent for acidification fracturing: A review. Geoenergy Sci. Eng. 247, 213600. https://doi.org/10.1016/j.geoen.2024.213600.

Zhu, D.Y., Fang, X.Y., Sun, R.X., et al., 2021a. Development of degradable preformed particle gel (DPPG) as temporary plugging agent for petroleum drilling and production. Pet. Sci. 18, 479–494. https://doi.org/10.1007/s12182-020-00535-w.

Zhu, D.Y., Xu, Z.H., Sun, R.X., et al., 2021b. Laboratory evaluation on temporary plugging performance of degradable preformed particle gels (DPPGs). Fuel 289, 119743. https://doi.org/10.1016/j.fuel.2020.119743.

Zhu, D.Y., Gong, Y.L., Wang, J.F., et al., 2023. Effect of crosslinker types on temporary plugging performance of degradable preformed particle gels for unconventional petroleum reservoir development. Energy Fuels 37, 373–384. https://doi.org/10.1021/acs.energyfuels.2c03915.

Zou, C.W., Dai, C.L., Liu, Y.F., et al., 2023. A novel self-degradable gel (SDG) as liquid temporary plugging agent for high-temperature reservoirs. J. Mol. Liq. 386, 122463. https://doi.org/10.1016/j.molliq.2023.122463.